molecular pharmaceutics

Article

pubs.acs.org/molecularpharmaceutics

Redox Potential Ultrasensitive Nanoparticle for the Targeted Delivery of Camptothecin to HER2-Positive Cancer Cells

Remant Bahadur K.C.,[†] Varun Chandrashekaran,[‡] Bei Cheng,[†] Hexin Chen,[‡] Maria Marjorette O. Peña,[‡] Jiajia Zhang,[§] Janis Montgomery,[∥] and Peisheng Xu*[,†]

[†]Department of Drug Discovery and Biomedical Sciences, South Carolina College of Pharmacy, University of South Carolina, 715 Sumter Street, Columbia, South Carolina 29208, United States

[‡]Department of Biological Sciences, University of South Carolina, 715 Sumter Street, Columbia, South Carolina 29208, United States

[§]Department of Epidemiology and Biostatistics, University of South Carolina, 800 Sumter Street, Columbia, South Carolina 29208, United States

[∥]South Carolina Oncology Associates, 166 Stoneridge Drive, Columbia, South Carolina 29210, United States

Supporting Information

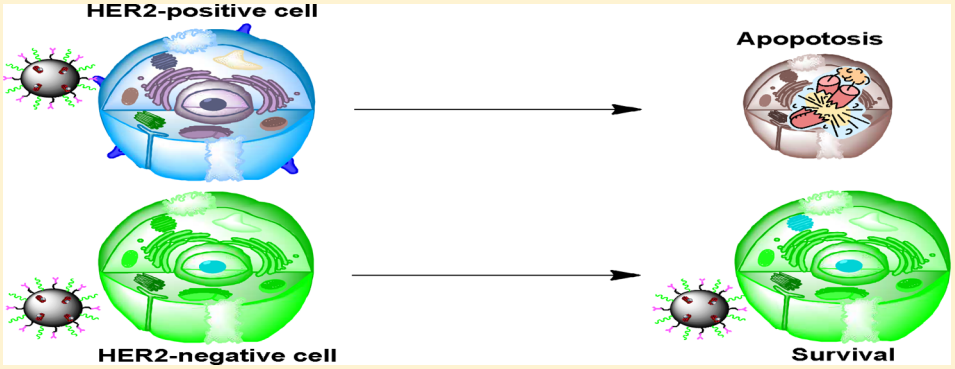

ABSTRACT: Ideal "smart" nanoparticles for drug delivery should enhance therapeutic efficacy without introducing side effects. To achieve that, we developed a drug delivery system (HCN) based on a polymer−drug conjugate of poly[2-(pyridin-2-yldisulfanyl)]-*graft*-poly(ethylene glycol) and camptothecin with an intracellularly cleavable linker and human epidermal growth factor receptor 2 (HER2) targeting ligands. An *in vitro* drug release study found that HCN was stable in the physiological environment and supersensitive to the stimulus of elevated intracellular redox potential, releasing all payloads in less than 30 min. Furthermore, confocal microscopy revealed that HCN could specifically enter HER2-positive cancer cells. As a consequence, HCN could effectively kill HER2-positive cancer cells while not affecting HER2-negative cells.

KEYWORDS: *redox sensitive, polymer−drug conjugate, HER2-positive, drug delivery, camptothecin*

1. INTRODUCTION

Nanoparticles with the capacity to increase drug solubility, stability, and specificity and, therefore, achieve enhanced therapeutic efficacy and attenuated off-target side effects have been explored extensively for the treatment of various types of diseases. Nanoparticulate drug carriers include micelles,[1,2] liposomes,[3,4] polymer−drug conjugates,[5,6] dendrimers,[7,8] and inorganic particles.[9,10]

Generally, a drug/small molecule can be loaded in a nanocarrier either by being encapsulated in a core with a similar hydrophobicity or by being conjugated through covalent bonds. For instance, hydrophobic drug doxorubicin can be conveniently encapsulated into the hydrophobic domain of a micelle fabricated from amphiphilic copolymers[11] or conjugated to water-soluble polymers via various bonds.[5,12] Correspondingly, the loaded doxorubicin can be released from the carrier by diffusion, the erosion of the carrier, or both, or via the breakage of the linker. Depending on the requirements of their applications, the extended drug release can decrease the dosing frequency, while the stimulus responsive drug release can potentially attenuate drug side effects.

Although tremendous efforts have been devoted to the development of nanomedicine for cancer chemotherapy, how to safely deliver active drugs into targeted cancer cells and kill them remains a challenge. There are at least two prerequisites for a safe nanocarrier: (i) a nanocarrier should be free of premature release before reaching its targeted cells, and (ii) the nanocarrier should enter only target cells. Because conventional encapsulation approaches are commonly associated with burst

Received: January 17, 2014
Revised: April 23, 2014
Accepted: April 29, 2014
Published: April 29, 2014

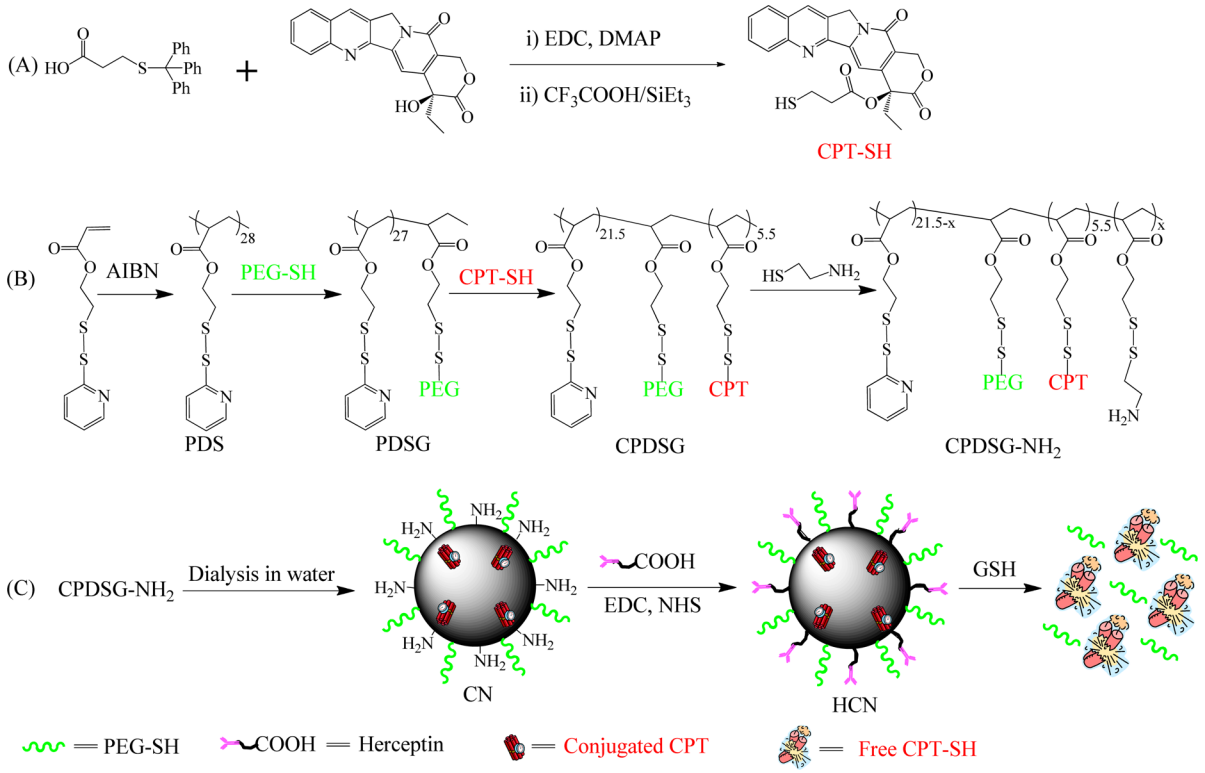

Figure 1. Syntheses of thiolated camptothecin (CPT-SH) (A) and the polymer−drug conjugate (CPDSG-NH_2) (B) and fabrication of a camptothecin nanoparticle (CN) and a Herceptin-functionalized camptothecin nanoparticle (HCN) (C).

release due to the detachment of a surface-adsorbed payload,[13,14] polymer−drug conjugates have attracted more and more attention recently because they can potentially eliminate the off-target effects by preventing initial burst release.

An effective polymer−drug conjugate-based intracellular nanocarrier should have the following features. They must (i) be made from an intracellular cleavable polymer−drug conjugate, which allows the nanoparticle to be stable under extracellular physiological conditions while unloading all payloads in a very short period of time due to the cleavage of the linker by intracellular stimuli; (ii) contain "stealth" poly(ethylene glycol) (PEG) blocks, which can extend the circulation time of nanocarriers by preventing opsonization and protecting them from being captured by the mononuclear phagocytic system (MPS);[15] and (iii) be functionalized with a targeting ligand that can specifically bind receptors overexpressed on the membrane of cancer cells. Hereby, with the help of redox potential sensitive disulfide bonds and Herceptin, a HER2 antibody, we designed a camptothecin−polymer conjugate-based micelle system for HER2-positive cancer therapy.

2. MATERIALS AND METHODS

2.1. Materials. Aldrithiol-2, camptothecin (CPT), and silica gel (spherical, 100 μm) were purchased from Tokyo Chemical Industry Co., Ltd. (Portland, OR). 2-Mercaptoethanol, DL-dithiothreitol (DTT), doxorubicin (DOX), thiazolyl blue tetrazolium bromide (MTT), 2,2-azobis(isobutyronitrile) (AIBN), and cysteamine hydrochloride were purchased from Sigma-Aldrich (St. Louis, MO). PEG-SH (mPEG-SH) (MW = 5000 Da) was purchased from Laysan Bio, Inc. (Arab, AL). 3-(Tritylthio)propionic acid was obtained from Santa Cruz Biotechnology (Santa Cruz, CA). Trypsin-EDTA, penicillin, streptomycin, Dulbecco's modified Eagle's medium (DMEM), and fetal bovine serum (FBS) were obtained from American Type Culture Collection (ATCC, Manassas, VA). Herceptin was acquired from Roche. All the other solvents used in this research were purchased from Sigma-Aldrich and used without any further purification unless otherwise noted.

2.2. Synthesis of Poly[2-(pyridin-2-yldisulfanyl)]-*graft*-poly(ethylene glycol) (PDSG). Poly[2-(pyridin-2-yldisulfanyl)] (PDS) was synthesized by free radical polymerization of 2-(pyridin-2-yldisulfanyl)ethyl acrylate (PDSA) using AIBN as an initiator (Figure 1). Briefly, 500 mg (2.7 mmol) of PDSA was dissolved in 10 mL of anisole into a 100 mL round-bottom flask and degassed for 30 min at room temperature. After that, 0.09 mmol of the AIBN anisole solution was added to the mixture. Then the flask was immersed in an oil bath maintained at 65 °C and stirred for 24 h. The resulting product was collected by precipitation (three times) into ice-cold diethyl ether and dried under vacuum for 48 h at room temperature. The structural composition of the polymer was analyzed by ^{1}H nuclear magnetic resonance (NMR) (Mercury Varian 400 NMR, Varian Inc., Palo Alto, CA) using $CDCl_3$ as a solvent and TMS as an internal standard. The molecular weight (M_w) and polydispersity of PDS were characterized by GPC (Viscotek GPCmax VE 2001 GPC solvent/sample module, Viscotek VE 3580 RI detector, and 270 dual detector) using tetrahydrofuran (THF) as the mobile phase. The PDS polymer was modified to yield an amphiphilic polymer by grafting PEG through the thiol−disulfide exchange reaction. Briefly, the PDS polymer (50 mg, 7.14 μmol) was dissolved in 5 mL of methylene chloride and mixed with 2 mL of a mPEG-SH (50 mg, 10 μmol, MW of 5 kDa) solution, and the solution was stirred for 12 h at room temperature. The progress of the reaction was evidenced by the appearance of a yellow color. The final product was precipitated

(three times) in ice-cold diethyl ether and vacuum-dried for 48 h to yield PDSG.

2.3. Chemical Modification of CPT and Conjugation onto PDSG. Thiolated CPT was synthesized according to the procedure described in the literature.[16] The modification was confirmed by ^{1}H NMR and HPLC [Waters model 2695 attached to a Waters 2996 photodiode array detector and column (C18, dimensions of 25 cm × 4.6 mm)] using a 1:1 (v/v) acetonitrile/water mixture [supplemented with 0.1% trifluoroacetic acid (TFA)] as the mobile phase. The eluted samples were detected at 375 nm (λ). The CPT-grafted PDSG polymer (CPDSG) was prepared by the thiol−disulfide exchange reaction between CPT-SH and the PDSG polymer (Figure 1). Briefly, PDSG (50 mg) was dissolved in dimethylformamide (DMF) (2 mL) and mixed with CPT-SH (10 mg in 1 mL of DMF). The reaction was conducted at room temperature for 12 h. The final product was precipitated (three times) in ice-cold ether and dried under vacuum for 48 h. ^{1}H NMR (Figure S1 of the Supporting Information), and HPLC confirmed the formation of the CPT−polymer conjugate. The critical micelle concentration of the CPDSG polymer was determined by fluorescence spectroscopy.[17]

2.4. Preparation, Functionalization, and Characterization of Nanoparticles. Polymer−drug conjugate-based micelle nanoparticles of CPDSG were prepared in PBS by the cosolvent dialysis method. Briefly, CPDSG (2 mg in 200 μL of DMSO) was dropped into 2 mL of ddH_2O while it was being stirred and equilibrated for 30 min. Then the solution was dialyzed (three times) using a Spectra/Por dialysis tube [molecular weight cutoff (MWCO) of 1.0 kDa] against PBS for 8 h, and the nanoparticles were collected and analyzed. For surface functionalization, CPDSG (2 mg) was reacted with cysteamine hydrochloride (200 μg) in 500 μL of a dichloromethane/methanol mixture [1:1 (v/v)] for 3 h at room temperature. After that, the solvent was removed under vacuum, and the residue was redissolved in DMSO (100 μL) and dropped into 2 mL of ddH_2O while it was being stirred. The nanoparticle solution was dialyzed (three times) through a Spectra/Por dialysis tube (MWCO of 1.0 kDa) against phosphate buffer (pH 8.0) for 8 h to yield CN (Figure 1C). PDS and PDSG nanoparticles were fabricated directly from PDS and PDSG polymers in parallel as a control. To endow CN with the specific targeting effect for HER2-positive cancer cells, CN was further functionalized with a HER2 antibody, Herceptin (Roche), at a ratio of 50 Herceptin molecules/CN with the help of 1-ethyl-3-[3-(dimethylamino)propyl]-carbodiimide (EDC) and *N*-hydroxysuccinimide (NHS) to yield HCN. Unreacted Herceptin was removed from the nanoparticle solution by Sephadex column filtration (three times) using PBS as a mobile phase. The morphology, size distribution, and surface charge (ζ potential) of the CPDSG nanoparticles (CN) or CPDSG−Her nanoparticles (HCN) were studied via transmission electron microscopy (TEM) using a Hitachi H-800 instrument operated at an accelerating voltage of 200 kV and dynamic light scattering (DLS) (Malvern Zetasizer, Nano-ZS). For TEM, the nanoparticle solution (1.0 mg/mL) was dropped on a carbon-coated copper grid and dried using tissue paper, and the images were taken without any further processing. DLS measurements were taken using a 1.0 mg/mL nanoparticle solution in PBS.

2.5. *In Vitro* Drug Release Study. *In vitro* release of the drug from CN was performed in PBS (pH 7.4) with and without DTT at 37 °C using a Spectra/Por dialysis bag (MWCO of 1.0 kDa). Three milliliters of a CN solution (~200 μg of CPT) was transferred into the tubing and immersed in PBS buffer (40 mL). One hundred microliters of the solution from the bag was sampled at different time intervals, and the same amount of fresh buffer was replaced to keep the volume constant. After dialysis for 24 h, DTT (final concentration of 10 mM) was added to the release buffer, which was then sampled every 10 min for an additional 6 h. Finally, the samples were lyophilized and redissolved in 1 mL of a DMSO/ddH_2O mixture [1:1 (v/v)], and the content of CPT-SH was quantified via HPLC as described above.

2.6. Cell Culture. Cancer cells, HCT-116 and KB cells, obtained from ATCC were maintained as a monolayer culture in Dulbecco's modified Eagle's medium (DMEM) supplemented with 10% fetal bovine serum (FBS) and 100 units/mL penicillin-streptomycin at 37 °C under a humidified atmosphere of 95% air and 5% CO_2. Cells were subcultured when the confluence reached 75%, and the medium was replaced every other day.

2.7. Western Blot of HER2. The cells were lysed in 1× TritonX lysis buffer at 80% confluence with 1× sodium orthovanadate (Alfa aesar) and 1× proteinase inhibitor (Roche). The lysate was then sonicated for 60 s on ice. The lysate was centrifuged at 13000 rcf for 10 min at 4 °C. The protein lysate was then quantified by the BCA method (Thermo Scientific), and equal concentrations of proteins were mixed with Laemmli buffer and loaded onto a gradient polyacrylamide gel (4 to 14%) from Bio-Rad. The gel was run at 100 V for 60 min. The proteins were then transferred onto a nitrocellulose membrane. The membrane was blocked using 5% blotting grade milk (Bio-Rad) for 45 min. After a brief wash with 1× phosphate-buffered saline Tween 20 (PBST), the primary antibody was added to the membrane at 1:5000 HER2 (Cell Signaling) and 1:1000 GAPDH (Santa Cruz) dilutions. The membranes were incubated with the antibody for 90 min at room temperature on a shaker. After incubation, the membranes were washed with 1× PBST three times. The membranes were then incubated in the HRP-conjugated secondary antibody at a 1:4000 dilution (GE) for 1 h at room temperature to detect target protein. After incubation, the membranes were washed with 1× PBST three times. Signals were detected using an ECL kit (Amersham Biosciences) and recorded on X-ray film (Phenix).

2.8. Cellular Uptake of HCN. Cellular uptake of the CPDSG nanoparticles was observed using confocal microscopy. To produce the fluorescence signal for the detection of nanoparticles, doxorubicin was encapsulated in CN or HCN during the fabrication of nanoparticles as described in our previous report.[18] HCT-116 and KB cells (2×10^5 cells/well) was seeded in 35 mm^2 glass-bottom dishes (MatTek) and grown overnight. The medium were replaced with medium (supplemented with 10% FBS) containing the nanoparticle solution (final DOX concentration of 5 μM) and incubated for 3 h. Then the cells were washed (three times) with prewarmed PBS, fixed for 25 min with formaldehyde (3.5% in PBS), and washed (three times) with PBS, and the nuclei were counterstained with Hoechst 33342 (final concentration of 1 μg/mL) for 5 min. Finally, the cells were washed (three times) with PBS and analyzed under a confocal microscope (LSM 510, Carl-Zeiss Inc., Oberkochen, Germany).

2.9. Flow Cytometry. To prepare Cy3-labeled CN, Cy3-NHS was incubated with CN in PBS for 2 h at room temperature. Then the unconjugated Cy3 was removed by gel

filtration chromatography using Sephadex 25 (three times). Cy3-labeled HCN was prepared similarly by adding Cy3-NHS to the CN suspension before the addition of activated Herceptin as described in section 2.4. Cells were seeded at a density of 3.5×10^5 cells/well in 12-well plates. After being grown overnight, cells were incubated with different treatment groups (CN and HCN) for 4 h at a concentration of 1.8 μg/mL for Cy3. Trypsin was used to detach the cells from the plate, and the cells were collected by centrifugation and then redispersed with 500 μL of PBS. Flow cytometry was then performed with a BD Accuri C6 instrument. In all FACS analysis, cell debris and free particles were excluded by setting a gate on the plot of side-scattered light (SSC) versus forward-scattered light (FSC). A total of 10000 gated cells were analyzed.

2.10. Anticancer Activity of HCN. Anticancer activities of CN and HCN nanoparticles were studied in different cancer cells (HCT-116 and KB cells) in 96-well microplates. Serial dilutions of the nanoparticles with a corresponding camptothecin concentration from 0.5 to 20 μM were prepared in culture medium supplemented with 10% FBS, and 150 μL of each concentration was directly added to the cells and incubated for 24 h in a 95:5 air/CO_2 mixture at 37 °C. The medium was replaced with fresh medium, and the cells were grown for an additional 24 h. Then the medium was replaced with 100 μL of medium containing MTT reagent (final concentration of 0.1 mg/mL) and incubated for 3 h. MTT crystals were dissolved with 100 μL of a MTT stop solution (20% SDS in DMF and water at a 1:1 ratio and 2% acetic acid) by incubation for 4 h at room temperature, and the optical density was measured (λ = 595 nm) using a microplate reader (EL_X808, Bio-Tech Instrument, Inc.). Cell viability was expressed relative to the reference control (untreated cell).

3. RESULTS

3.1. Synthesis of the PDSG Polymer. Because of its easy postpolymerization functionalization,[19] the PDS polymer built from pyridyldisulfide-functionalized acrylate monomers was adopted and synthesized by free radical polymerization according to our published protocol (M_w = 7.1 kDa; PDI = 1.45).[20] Thiolated poly(ethylene glycol) (PEG5000-SH) was conjugated to the PDS polymer to yield the amphiphilic PDS–PEG copolymer (PDSG) via thiol–disulfide exchange. The emergence of the proton peak at 3.6 ppm in the ^{1}H NMR spectrum after PEG conjugation proved the formation of PDSG (Figure S1 of the Supporting Information). The right shifting of the gel permeation chromatography (GPC) curve (retention volume decreased from 9.4 to 8.65 mL) further confirmed the grafting of PEG to PDS (Figure S2 of the Supporting Information). The shallow shoulder in the GPC curve of PDSG indicated the presence of a small portion of unreacted PDS. The molecular weight of PDSG was 11.9 kDa (PDI of 1.38) as determined by GPC, suggesting each PDSG polymer chain contained approximately one PEG molecule.

3.2. Synthesis of CPT-SH and CPDSG. The hydrophobic anticancer drug camptothecin (CPT) was thiolated (Figure 1A) and then grafted onto the PDSG polymer to form CPDSG through thiol–disulfide exchange (Figure 1B). Researchers have confirmed that thiolation of CPT does not significantly affect its anticancer efficacy.[6,21] The successful yield of thiolated CPT (CPT-SH) was confirmed by ^{1}H NMR, HPLC, and mass spectroscopy. The ethylene proton resonance peaks corresponding to CPT at δ = 1.85 ppm slightly shifted to δ = 2.2 ppm. Along with the characteristic proton peaks of CPT, a new ethyl proton peak (δ = 2.84 ppm) was clearly visible in the ^{1}H NMR spectra (Figure S1 of the Supporting Information). The change in the chemistry of CPT after thiolation and conjugation onto the polymer was also observed in the HPLC chromatogram. The retention time of CPT significantly shifted from 3.2 to 8.0 min after thiolation (Figure 2B). HPLC

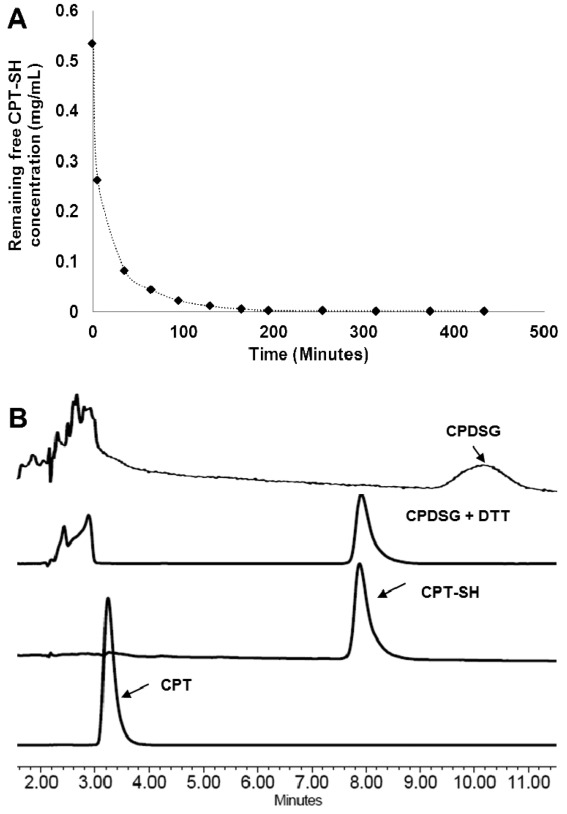

Figure 2. Reaction kinetics of CPT-SH conjugation (A) and HPLC spectra of CPT, CPT-SH, and CPT-conjugated polymer (CPDSG) and the release of CPT-SH from CPDSG in an environment containing 10 mM DTT (B).

was also employed to monitor the CPT conjugation process by quantifying the remaining free CPT-SH and showed that 3.5 h was enough to complete the reaction and achieve 100% conjugation efficiency (Figure 2A). HPLC spectra evidenced the successful conjugation of CPT onto PDSG, an emerging peak with an elution time of 10.5 min (Figure 2B). The amount of CPT-SH selected for the preparation of CPDSG was optimized by incubating different amounts of CPT-SH with polymer, and 20% (w/w) CPT-SH was selected for the study based on the balancing between high drug loading content and appropriate particle size formed thereafter. The feeding ratio for grafting CPT-SH onto PDSG was 5:1 [repeating unit of PDS/CPT-SH (molar ratio)]. Because no residual CPT-SH signal was observed during HPLC for the CPDSG reaction product (see the spectrum of CPDSG in Figure 2B), each polymer should have around six CPT-SH molecules grafted. To evaluate the ability of CPT-SH to be released from the CPDSG polymer in a reducing environment, 10 mM dithiothreitol (DTT) was added to the CPDSG polymer DMSO solution. As expected, HPLC showed that all conjugated CPT-SH could be liberated from CPDSG as evidenced by the complete disappearance of the absorbance peak at 10.5 min and the recovery of the peak at

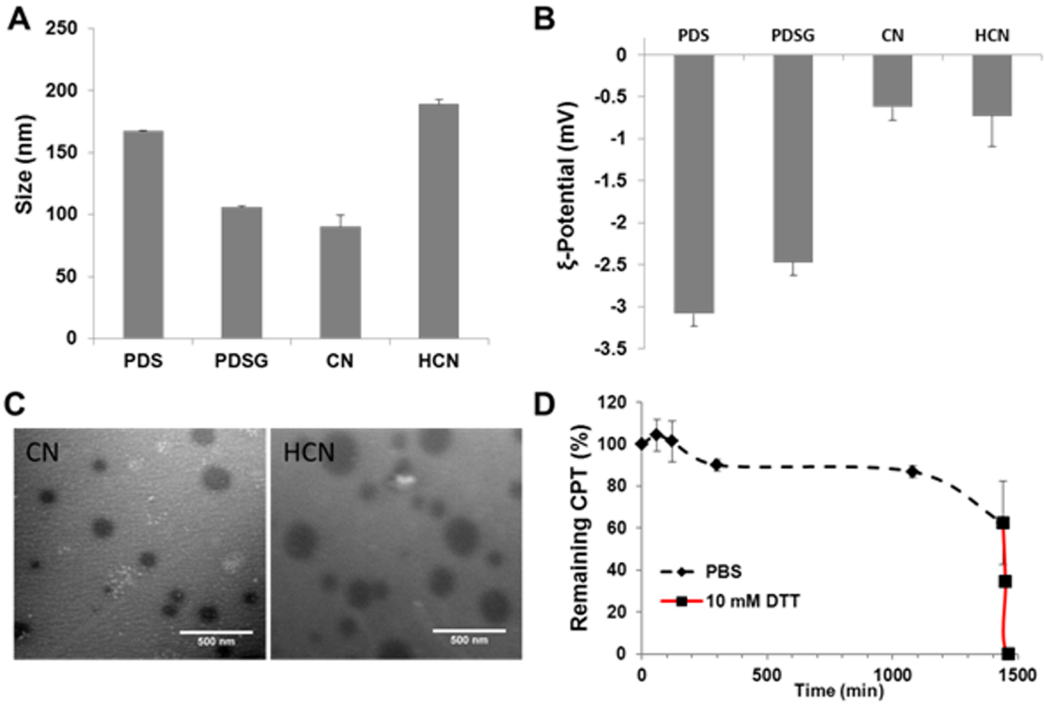

Figure 3. Hydrodynamic size (A), ξ potential (B), and TEM images (C) of nanoparticles and the kinetics of release of CPT-SH from CN in different environments (D). Data represent means ± the standard deviation (n = 3). Scale bars are 500 nm in panel C.

8.0 min (Figure 2B). The critical micelle concentration of CPDSG was 12 μg/mL as determined by fluorescence spectroscopy (Figure S3 of the Supporting Information).

3.3. Fabrication and Characterization of CN and HCN Nanoparticles. Dynamic light scattering (DLS) and phase analysis light scattering (PALS) were employed to investigate the physicochemical characteristics of the nanoparticles prepared as described above. For the CPDSG polymer, PEG block is hydrophilic while both CPT and PDS are relatively hydrophobic. Because of the amphiphilicity of the polymer, CPDSG self-assembles into micelles with a core made of PDS as well as CPT, and PEG corona (Figure 1C). DLS revealed that the conjugation of PEG significantly reduced the size of PDS from 168 to 107 nm (Figure 3A). Because of the formation of a more condensed hydrophobic CPT core, CNs with a low CPT grafting ratio were smaller than PDSG. Our pilot study found that the size of CN increased proportionally with the increase in the CPT-SH grafting ratio. The goal for the CPT-SH loading optimization was to achieve a CN with the highest CPT loading content while keeping its size smaller than 100 nm. Via the optimization, a CN with a 16.7% CPT-SH loading content and a size of 85 nm was selected. CN was functionalized with Herceptin at a feeding ratio of 50 molecules per CN. The Bradford protein assay was conducted to evaluate the Herceptin conjugation efficiency. However, because of the relatively low concentration of Herceptin used and the interference of the nanoparticle, the absolute number of Herceptin molecules per nanoparticle could not be determined. CN doubled its size to 187 nm after Herceptin functionalization. Because the hydrodynamic size of Herceptin was <20 nm,[22] we postulate that the increased size (102 nm) was partially due to the cross-linking effect of Herceptin in addition to surface functionalization. Because of the contribution of pyridine groups, all nanoparticles were slightly negatively charged with ξ ranging from −3.08 ± 0.15 to −0.63 ± 0.15 mV (Figure 3B), suggesting that HCN could be a good carrier for targeted drug delivery because of its ability to escape detection by the MPS system.[23] The addition of PEG could further protect HCN from the capture of the MPS system as well as decrease the size of PDS and slightly attenuate the surface charge. TEM images revealed that both CN and HCN nanoparticles were spherical and further confirmed the size increase for HCN after Herceptin modification (Figure 3C).

3.4. Drug Release Kinetics of the Nanoparticle. Studies have revealed that the difference in redox potential level between the intracellular and extracellular environments is several orders of magnitude, <0.01 mM glutathione (GSH) for the extracellular fluid and 1−11 mM GSH for the cytoplasm.[24] To investigate the redox potential sensitivity of CN, DTT was employed instead of GSH because the addition of GSH would decrease the pH of the release buffer, which could potentially introduce false redox potential sensitivity. Nanoparticles were dialyzed against PBS and PBS supplemented with 10 mM DTT to mimic extracellular and intracellular environments, respectively. Figure 3D shows that before the addition of DTT only 38% of CPT-SH was released over 24 h. Then 10 mM DTT was added to mimic the intracellular reducing environment. To our surprise, the remaining 62% of CPT-SH was released in only 20 min, indicating that CN was supersensitive to the endogenous stimulus, a high redox potential.

3.5. Cytotoxicity of CN and HCN for HER2-Positive and -Negative Cells. HER2-positive cancers are generally aggressive and closely associated with poor prognostic outcome.[25] To endow CN with specificity in killing HER2-positive cancer cells, Herceptin, a HER2 antibody, was conjugated to the surface of CN to yield HCN. To investigate the selective cell killing effect of HCN, HER2-posivive HCT-116 colon cancer cells and HER2-negative KB cells were treated with CN and HCN for 48 h and evaluated by the MTT assay. Western immunoblotting analysis confirmed the

dx.doi.org/10.1021/mp5000482 | Mol. Pharmaceutics 2014, 11, 1897−1905

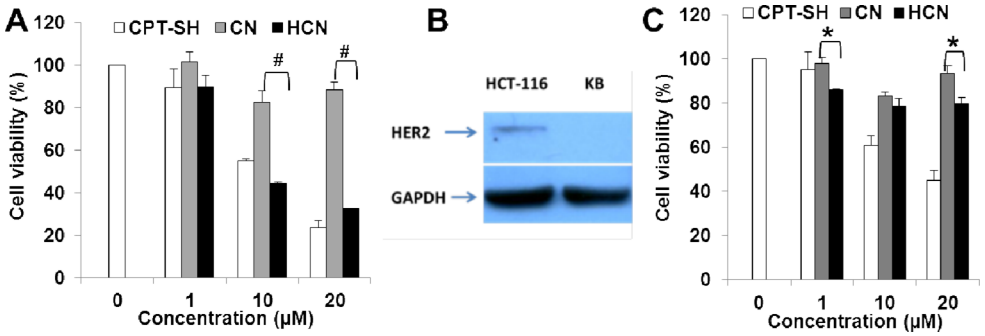

Figure 4. Cytotoxicity of CN and HCN for HER2-positive HCT-116 cells (A) and HER2-negative KB cells (C) after treatment for 48 h and Western blotting of HER2 expression in HCT-116 and KB cells (B). Data represent means ± the standard deviation (n = 3) (Student's t test; $^{*}P < 0.05$; $^{\#}P < 0.01$).

expression of HER2 in HCT-116 but not in KB cells (Figure 4B). Panels A and C of Figure 4 show that thiolated CPT (CPT-SH) retained its anticancer activity and exhibited dose responsive inhibition of proliferation for both cell lines, which is consistent with the reports of others.[21] The MTT assay also revealed that CN was almost nontoxic for both HCT-116 and KB cells, killing less than 12 and 7% of the HCT-116 and KB cells, respectively, at the equivalent CPT-SH concentration of 20 μM, at which free CPT-SH killed more than 80 and 50% of the cells, respectively. This suggested that the premature release of CPT from CN ranged from minimal to none. Unlike CN, HCN exhibited a potency similar to that of free CPT-SH in killing HER2-positive HCT-116 cells; ~68% of the cells were killed after the HCN treatment at a concentration of 20 μM. To our surprise, HCN barely killed HER2-negative KB cells (only ~20% of the cells were killed at a concentration of 20 μM), suggesting that HCN did highly selectively inhibit the growth of HER2-positive cancer cells. To examine whether this HER2 specific cell killing was solely due to the inhibitory effect of Herceptin, a HER2 antibody used clinically for the treatment of HER2-positive breast cancer, a MTT assay was conducted to measure the cell viability after treatment with Herceptin at concentrations of 0.1−8.7 μg/mL. Figure 5A shows that Herceptin was nontoxic in the tested concentration range. Because the corresponding Herceptin dose in HCN at a CPT-SH concentration of 20 μM was 2.4 μg/mL, which was less than 8.7 μg/mL and far less than its clinical concentration, we think that the HER2 specific cell killing effect was due to Herceptin enhancing HCN uptake rather than the cell growth inhibitory effect of Herceptin itself. The MTT assay also proved that the PDSG polymer was not toxic for HCT-116 cells (Figure 5B).

3.6. Cellular Uptake of CN and HCN Nanoparticles. To investigate how HCN achieved a selective killing effect for HER2-positive cells, the cellular uptake of nanoparticles was observed via laser scanning confocal microscopy. Doxorubicin (DOX), an anticancer drug that is also a convenient fluorescent probe, was encapsulated into CN and HCN. The addition of DOX into CN and HCN slightly decreased their hydrodynamic size (~5 nm). There was no difference in surface charge between the CNs or HCNs with and without doxorubicin encapsulation. After treatment for 3 h, there were only very dim red fluorescent signals shown in both cell lines treated with CN (Figure 6), indicating that CN had hardly been taken up by either cell line. As expected, a much stronger red fluorescent signal appeared in HCN-treated HCT-116 cells than in CN-treated ones. However, there was no observable increase of the

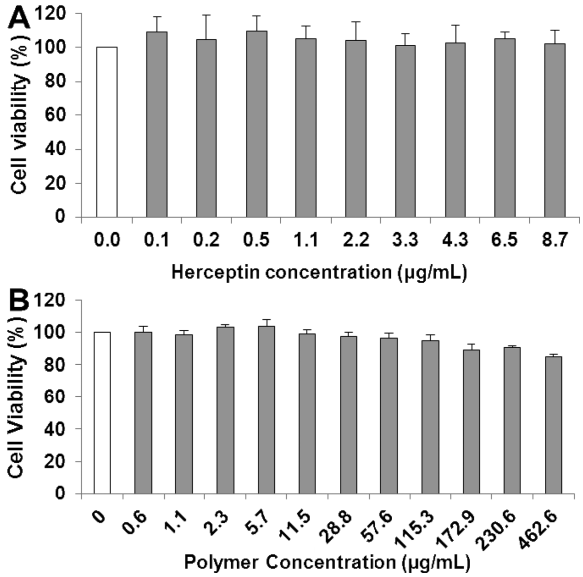

Figure 5. Cytotoxicity of Herceptin (A) and PDSG (B) for HER2-positive HCT-116 cells after treatment for 48 h. Data represent means ± the standard deviation (n = 3).

red fluorescent signal in KB cells cocultured with HCN, suggesting that HCN can effectively enter only HER2-positive cells, not HER2-negative ones. Flow cytometry data (Figure 6C,D) further revealed that the addition of Herceptin to CN did significantly enhance its entry into HCT-116 cells (HER-positive cells) but not KB cells (HER-negative cells).

4. DISCUSSION

To achieve a specific cell killing effect, a drug carrier system should meet at least the following three conditions. First, the loaded drug should be released only after entering the targeted cell. Second, the drug released from the carrier should remain active. Third, the carrier can be taken up by only its targeted cells. Disulfide bonds have been incorporated into various drug carriers with the aim of achieving a desired stability during circulation and quick release in a reducing intracellular environment because of the high GSH concentration.[18,20,26−28]

In our design, CPT was conjugated onto the PDSG polymer through thiol−disulfide exchange reaction via disulfide bond linkage to realize intracellular release. Because PEG is hydrophilic while both CPT and PDS segments are hydrophobic, CPDSG self-assembled into the nanoparticle CN in an aqueous solution (Figure 3C). The PDS polymer is

dx.doi.org/10.1021/mp5000482 | Mol. Pharmaceutics 2014, 11, 1897−1905

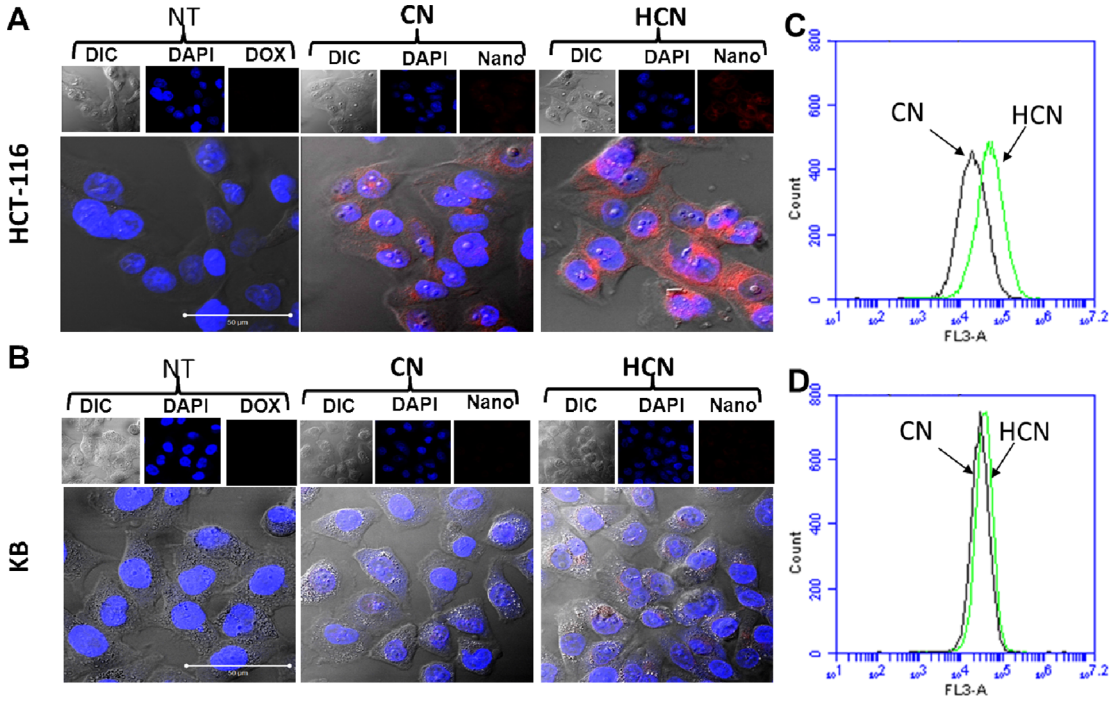

Figure 6. Confocal images and flow cytometry spectra of HCT-116 cells (A and C) and KB cells (B and D) treated with CN and HCN nanoparticles. Doxorubicin was encapsulated into CN and HCN nanoparticles as a fluorescence reporter (red, DOX); nuclei of the cells were stained with Hoechst 33342 (blue, DAPI) (A and B). Cells were cocultured with Cy3-labeled CN and HCN (C and D) for 4 h.

biodegradable and can be degraded through the hydrolysis of ester bonds at acidic pH (inside the lysosomes) and the cleavage of disulfide bonds (in reducing cytosol). The molecular weight of PDS will decrease to <3000 Da after the cleavage of all side chains, which can be easily excreted from the body by renal clearance. Figure 3D proves that in a buffer with no reducing agent CPT-SH could be only slowly released (38% released in 24 h). As a consequence, the off-target effect induced by premature release would be significantly reduced. Cell killing results shown in panels A and C of Figure 4 also revealed that. HPLC demonstrated that CPT-SH could be released from CN without any modification (Figure 2B). Furthermore, the MTT assay showed that CPT-SH was still active in killing cancer cells (Figure 4), which is consistent with the literature report.[8,24] Figure 6 validates that without the help of targeting ligand CN could enter neither HER2-positive nor HER2-negative cells. Confocal microscopy also verified that Herceptin modification facilitated the entry of HCN into only HER2-positive cells, not HER2-negative ones. Flow cytometry data further proved that the modification of Herceptin to CN facilitated the entry of HCN into HCT-116 cells, not KB cells (Figure 6C,D). Moreover, Figure 3D also confirmed that CPT-SH could be liberated from the nanoparticle in a superfast manner under conditions similar to those of the intracellular environment (62% in 20 min), suggesting CN was far more sensitive to the reducing environment than other developed redox potential sensitive systems, which generally need several hours to release all payloads.[29,30] The difference in cell viability between two cell lines was only observed in HCN and not CN treatment, indicating the observed cell type specific killing effect was not caused by the difference in free thiols produced in the culture media between two cell lines. The integration of the characteristics of HCN mentioned above endows it with the ability to specifically kill HER2-positive cancer cells, as shown in Figure 4.

HER2 is overexpressed in approximately 20−30% of invasive breast cancer and is associated with poor disease-free survival and poor response to chemotherapy.[31,32] One of the significant advances in the application of monoclonal antibodies in oncology was the introduction and approval of Herceptin, a humanized anti-HER2 antibody, for the treatment of HER2-positive breast cancer and HER2-positive metastatic gastric or gastresophageal junction adenocarcinoma.[33] Despite initial successes and encouraging results, the development of monoclonal antibody-based therapies faces several challenges.[34] Up to 74% of HER2-positive breast cancer patients are resistant to anti-HER2 antibody Herceptin,[35] and a majority of patients with HER2-positive breast cancer develop acquired resistance within one year.[36] A majority of these Herceptin-resistant cells still overexpress HER2, suggesting that resistance to Herceptin is not due to the loss of HER2 overexpression.[37,38] The Herceptin-conjugated nanoparticle developed in this study may provide a unique system that can be used to specifically deliver therapeutic drugs to HER2-positive cancer cells regardless of their response to Herceptin treatment.

In addition, in response to chemotherapy, cancer cells can develop multidrug resistance (MDR); mechanisms for this include compartmentalization, enhanced metabolism, and efflux pumps.[39] The P-glycoprotein (P-gp) pump (efflux pump) can remove drug molecules from the cytoplasm and decrease the intracellular drug concentration to a level lower than its effective dose, which is the primary reason for the failure of chemotherapy. To overcome the MDR effect, an effective drug carrier should have the ability to quickly release its payload intracellularlly to saturate the processing capacity of P-gp pumps. Because HCN could discharge all payloads in 20 min, it offers a novel approach for eradicating drug-resistant cancer cells.

dx.doi.org/10.1021/mp5000482 | *Mol. Pharmaceutics* 2014, 11, 1897−1905

5. CONCLUSIONS

A HER2-targeted nanoparticle, HCN, has been developed using the polymer−drug conjugates of PDSG and camptothecin. The release kinetic study found that HCN was supersensitive to the trigger of elevated redox potential, a characteristic of the intracellular environment, releasing all payloads in less than 30 min. With the help of HER2 antibody Herceptin, HCN could specifically enter HER2-positive cells and exclusively kill them. Because of its supersensitivity to the intracellular environment, HCN could open a new paradigm in overcoming MDR of cancer.

■ ASSOCIATED CONTENT

Ⓢ Supporting Information

^{1}H NMR spectra of CPT-SH, PDSG, and CPDSG (Figure S1), GPC spectra of PDS and PDSG (Figure S2), and critical micelle concentration measurements (Figure S3). This material is available free of charge via the Internet at http://pubs.acs.org.

■ AUTHOR INFORMATION

Corresponding Author

*E-mail: xup@sccp.sc.edu. Phone: (803) 777-0075. Fax: (803) 777-8356.

Notes

The authors declare no competing financial interest.

■ ACKNOWLEDGMENTS

We are thankful for the American Cancer Society Institutional Research Grant (ACS-IRG), the ASPIRE award from the Office of the Vice President for Research of The University of South Carolina, the Center for Colon Cancer Research (5 P20 RR017698), and the New Investigator Awards Program from the American Association of College of Pharmacy (AACP) for financial support to P.X. This work was also partly supported by an American Cancer Society Research Award (RSG-10-067-01-TBE) to H.C.

■ ABBREVIATIONS

AIBN, 2,2-azobis(isobutyronitrile); CPT, camptothecin; CN, camptothecin nanoparticle; CPT-SH, thiolated camptothecin; DLS, dynamic light scattering; DMEM, Dulbecco's modified Eagle's medium; DMF, dimethylformamide; DMSO, dimethyl sulfoxide; DTT, DL-dithiothreitol; DOX, doxorubicin; EDC, 1-ethyl-3-[3-(dimethylamino)propyl]carbodiimide; FBS, fetal bovine serum; GPC, gel permeation chromatography; GSH, glutathione; HCN, Herceptin-functionalized camptothecin nanoparticle; HER2, human epidermal growth factor receptor 2; MDR, multidrug resistance; MPS, mononuclear phagocytic system; MTT, thiazolyl blue tetrazolium bromide; NHS, *N*-hydroxysuccinimide; PALS, phase analysis light scattering; PBS, phosphate-buffered saline; PBST, phosphate-buffered saline Tween 20; PDSA, 2-(pyridin-2-yldisulfanyl)ethyl acrylate; PDSG, poly[2-(pyridin-2-yldisulfanyl)]-*graft*-poly(ethylene glycol); CPDSG, CPT-grafted PDSG; PDS, poly[2-(pyridin-2-yldisulfanyl)]; PEG, poly(ethylene glycol); P-gp, P-glycoprotein; SDS, sodium dodecyl sulfate; TEM, transmission electron microscopy; TFA, trifluoroacetic acid; THF, tetrahydrofuran

■ REFERENCES

(1) Master, A. M.; Rodriguez, M. E.; Kenney, M. E.; Oleinick, N. L.; Gupta, A. S. Delivery of the photosensitizer Pc 4 in PEG-PCL micelles for in vitro PDT studies. *J. Pharm. Sci.* **2010**, *99* (5), 2386−2398.

(2) Xu, P.; Van Kirk, E. A.; Murdoch, W. J.; Zhan, Y.; Isaak, D. D.; Radosz, M.; Shen, Y. Anticancer efficacies of cisplatin-releasing pH-responsive nanoparticles. *Biomacromolecules* **2006**, *7* (3), 829−835.

(3) Immordino, M. L.; Dosio, F.; Cattel, L. Stealth liposomes: Review of the basic science, rationale, and clinical applications, existing and potential. *Int. J. Nanomed.* **2006**, *1* (3), 297−315.

(4) Moreira, J. N.; Gaspar, R.; Allen, T. M. Targeting stealth liposomes in a murine model of human small cell lung cancer. *Biochim. Biophys. Acta* **2001**, *1515* (2), 167−176.

(5) Shi, M.; Ho, K.; Keating, A.; Shoichet, M. S. Doxorubicin-Conjugated Immuno-Nanoparticles for Intracellular Anticancer Drug Delivery. *Adv. Funct. Mater.* **2009**, *19* (11), 1689−1696.

(6) Zhou, Z.; Shen, Y.; Tang, J.; Fan, M.; Van Kirk, E. A.; Murdoch, W. J.; Radosz, M. Charge-Reversal Drug Conjugate for Targeted Cancer Cell Nuclear Drug Delivery. *Adv. Funct. Mater.* **2009**, *19* (22), 3580−3589.

(7) Guo, R.; Shi, X. Dendrimers in cancer therapeutics and diagnosis. *Curr. Drug Metab.* **2012**, *13* (8), 1097−1109.

(8) Menjoge, A. R.; Kannan, R. M.; Tomalia, D. A. Dendrimer-based drug and imaging conjugates: Design considerations for nanomedical applications. *Drug Discovery Today* **2010**, *15* (5−6), 171−185.

(9) Sun, T.-M.; Wang, Y.-C.; Wang, F.; Du, J.-Z.; Mao, C.-Q.; Sun, C.-Y.; Tang, R.-Z.; Liu, Y.; Zhu, J.; Zhu, Y.-H.; Yang, X.-Z.; Wang, J. Cancer stem cell therapy using doxorubicin conjugated to gold nanoparticles via hydrazone bonds. *Biomaterials* **2014**, *35* (2), 836−845.

(10) Shen, J.; Song, G.; An, M.; Li, X.; Wu, N.; Ruan, K.; Hu, J.; Hu, R. The use of hollow mesoporous silica nanospheres to encapsulate bortezomib and improve efficacy for non-small cell lung cancer therapy. *Biomaterials* **2014**, *35* (1), 316−326.

(11) Xu, P.; Van Kirk, E. A.; Zhan, Y.; Murdoch, W. J.; Radosz, M.; Shen, Y. Targeted charge-reversal nanoparticles for nuclear drug delivery. *Angew. Chem., Int. Ed.* **2007**, *46* (26), 4999−5002.

(12) Furgeson, D. Y.; Dreher, M. R.; Chilkoti, A. Structural optimization of a "smart" doxorubicin-polypeptide conjugate for thermally targeted delivery to solid tumors. *J. Controlled Release* **2006**, *110* (2), 362−369.

(13) Karavelidis, V.; Karavas, E.; Giliopoulos, D.; Papadimitriou, S.; Bikiaris, D. Evaluating the effects of crystallinity in new biocompatible polyester nanocarriers on drug release behavior. *Int. J. Nanomed.* **2011**, *6*, 3021−3032.

(14) Mohammadi, G.; Valizadeh, H.; Barzegar-Jalali, M.; Lotfipour, F.; Adibkia, K.; Milani, M.; Azhdarzadeh, M.; Kiafar, F.; Nokhodchi, A. Development of azithromycin-PLGA nanoparticles: Physicochemical characterization and antibacterial effect against *Salmonella typhi*. *Colloids Surf., B* **2010**, *80* (1), 34−39.

(15) Owens, D. E., III; Peppas, N. A. Opsonization, biodistribution, and pharmacokinetics of polymeric nanoparticles. *Int. J. Pharm.* **2006**, *307* (1), 93−102.

(16) Zhou, Z. X.; Shen, Y. Q.; Tang, J. B.; Fan, M. H.; Van Kirk, E. A.; Murdoch, W. J.; Radosz, M. Charge-Reversal Drug Conjugate for Targeted Cancer Cell Nuclear Drug Delivery. *Adv. Funct. Mater.* **2009**, *19* (22), 3580−3589.

(17) Xu, P.; Tang, H.; Li, S.; Ren, J.; Van Kirk, E.; Murdoch, W. J.; Radosz, M.; Shen, Y. Enhanced stability of core-surface cross-linked micelles fabricated from amphiphilic brush copolymers. *Biomacromolecules* **2004**, *5* (5), 1736−1744.

(18) K.C., R. B.; Thapa, B.; Xu, P. pH and redox dual responsive nanoparticle for nuclear targeted drug delivery. *Mol. Pharmaceutics* **2012**, *9* (9), 2719−2729.

(19) Gauthier, M. A.; Gibson, M. I.; Klok, H. A. Synthesis of functional polymers by post-polymerization modification. *Angew. Chem., Int. Ed.* **2009**, *48* (1), 48−58.

(20) K.C., R. B.; Xu, P. Multicompartment Intracellular Self-Expanding Nanogel for Targeted Delivery of Drug Cocktail. *Adv. Mater.* **2012**, *24* (48), 6479−6483.

(21) Shen, Y.; Zhou, Z.; Sui, M.; Tang, J.; Xu, P.; Van Kirk, E. A.; Murdoch, W. J.; Fan, M.; Radosz, M. Charge-reversal polyamidoamine

dendrimer for cascade nuclear drug delivery. *Nanomedicine (London, U.K.)* **2010**, *5* (8), 1205−1217.
(22) Demeule, B.; Palais, C.; Machaidze, G.; Gurny, R.; Arvinte, T. New methods allowing the detection of protein aggregates: A case study on trastuzumab. *mAbs* **2009**, *1* (2), 142−150.
(23) Xiao, K.; Li, Y.; Luo, J.; Lee, J. S.; Xiao, W.; Gonik, A. M.; Agarwal, R. G.; Lam, K. S. The effect of surface charge on in vivo biodistribution of PEG-oligocholic acid based micellar nanoparticles. *Biomaterials* **2011**, *32* (13), 3435−3446.
(24) Schafer, F. Q.; Buettner, G. R. Redox environment of the cell as viewed through the redox state of the glutathione disulfide/glutathione couple. *Free Radical Biol. Med.* **2001**, *30* (11), 1191−1212.
(25) Pradeep, C. R.; Zeisel, A.; Kostler, W. J.; Lauriola, M.; Jacob-Hirsch, J.; Haibe-Kains, B.; Amariglio, N.; Ben-Chetrit, N.; Emde, A.; Solomonov, I.; Neufeld, G.; Piccart, M.; Sagi, I.; Sotiriou, C.; Rechavi, G.; Domany, E.; Desmedt, C.; Yarden, Y. Modeling invasive breast cancer: Growth factors propel progression of HER2-positive premalignant lesions. *Oncogene* **2012**, *31* (31), 3569−3583.
(26) Ganta, S.; Devalapally, H.; Shahiwala, A.; Amiji, M. A review of stimuli-responsive nanocarriers for drug and gene delivery. *J. Controlled Release* **2008**, *126* (3), 187−204.
(27) Meng, F. H.; Hennink, W. E.; Zhong, Z. Reduction-sensitive polymers and bioconjugates for biomedical applications. *Biomaterials* **2009**, *30* (12), 2180−2198.
(28) Bae, Y.; Fukushima, S.; Harada, A.; Kataoka, K. Design of environment-sensitive supramolecular assemblies for intracellular drug delivery: Polymeric micelles that are responsive to intracellular pH change. *Angew. Chem., Int. Ed.* **2003**, *42* (38), 4640−4643.
(29) Pan, Y.-J.; Chen, Y.-Y.; Wang, D.-R.; Wei, C.; Guo, J.; Lu, D.-R.; Chu, C.-C.; Wang, C.-C. Redox/pH dual stimuli-responsive biodegradable nanohydrogels with varying responses to dithiothreitol and glutathione for controlled drug release. *Biomaterials* **2012**, *33* (27), 6570−6579.
(30) Luo, Z.; Cai, K.; Hu, Y.; Zhao, L.; Liu, P.; Duan, L.; Yang, W. Mesoporous Silica Nanoparticles End-Capped with Collagen: Redox-Responsive Nanoreservoirs for Targeted Drug Delivery. *Angew. Chem., Int. Ed.* **2011**, *50* (3), 640−643.
(31) Gusterson, B. A.; Gelber, R. D.; Goldhirsch, A.; Price, K. N.; Save-Soderborgh, J.; Anbazhagan, R.; Styles, J.; Rudenstam, C. M.; Golouh, R.; Reed, R.; et al. Prognostic importance of c-erbB-2 expression in breast cancer. International (Ludwig) Breast Cancer Study Group. *J. Clin. Oncol.* **1992**, *10* (7), 1049−1056.
(32) Slamon, D. J.; Godolphin, W.; Jones, L. A.; Holt, J. A.; Wong, S. G.; Keith, D. E.; Levin, W. J.; Stuart, S. G.; Udove, J.; Ullrich, A.; et al. Studies of the HER-2/neu proto-oncogene in human breast and ovarian cancer. *Science* **1989**, *244* (4905), 707−712.
(33) Shepard, H. M.; Jin, P.; Slamon, D. J.; Pirot, Z.; Maneval, D. C. Herceptin. *Handb. Exp. Pharmacol.* **2008**, *181*, 183−219.
(34) Yan, L.; Ehrlich, P. J.; Gibson, R.; Pickett, C.; Beckman, R. A. How can we improve antibody-based cancer therapy? *mAbs* **2009**, *1* (1), 67−70.
(35) Vogel, C. L.; Cobleigh, M. A.; Tripathy, D.; Gutheil, J. C.; Harris, L. N.; Fehrenbacher, L.; Slamon, D. J.; Murphy, M.; Novotny, W. F.; Burchmore, M.; Shak, S.; Stewart, S. J.; Press, M. Efficacy and safety of trastuzumab as a single agent in first-line treatment of HER2-overexpressing metastatic breast cancer. *J. Clin. Oncol.* **2002**, *20* (3), 719−726.
(36) Slamon, D. J.; Leyland-Jones, B.; Shak, S.; Fuchs, H.; Paton, V.; Bajamonde, A.; Fleming, T.; Eiermann, W.; Wolter, J.; Pegram, M.; Baselga, J.; Norton, L. Use of Chemotherapy plus a Monoclonal Antibody against HER2 for Metastatic Breast Cancer That Overexpresses HER2. *N. Engl. J. Med.* **2001**, *344* (11), 783−792.
(37) Diermeier, S.; Horvath, G.; Knuechel-Clarke, R.; Hofstaedter, F.; Szollosi, J.; Brockhoff, G. Epidermal growth factor receptor coexpression modulates susceptibility to Herceptin in HER2/neu overexpressing breast cancer cells via specific erbB-receptor interaction and activation. *Exp. Cell Res.* **2005**, *304* (2), 604−619.
(38) Ritter, C. A.; Perez-Torres, M.; Rinehart, C.; Guix, M.; Dugger, T.; Engelman, J. A.; Arteaga, C. L. Human breast cancer cells selected for resistance to trastuzumab in vivo overexpress epidermal growth factor receptor and ErbB ligands and remain dependent on the ErbB receptor network. *Clin. Cancer Res.* **2007**, *13* (16), 4909−4919.
(39) Gottesman, M. M. Mechanisms of cancer drug resistance. *Annu. Rev. Med.* **2002**, *53* (1), 615−627.